Correlating 3D light to 3D electron microscopy for systems biology

Collinson, LM; Carroll, Elizabeth; Hoogenboom, Jacob

DOI
10.1016/j.cobme.2017.10.006

Publication date
2017

Document Version
Accepted author manuscript

Published in
Current Opinion in Biomedical Engineering

Correlating 3D light to 3D electron microscopy for systems biology

Lucy M. Collinson[1], Elizabeth C. Carroll[2], Jacob P. Hoogenboom[2*]

[1]Electron Microscopy Science Technology Platform, Francis Crick Institute, London, UK

[2]Department of Imaging Physics, Delft University of Technology, Delft, the Netherlands

[*]Corresponding author: j.p.hoogenboom@tudelft.nl

Abstract

Whilst a 'resolution revolution' has taken place at the macromolecular scale in both electron microscopy and light microscopy, a 'volume revolution' has taken place at the tissue and organism level in both imaging modalities. At both ends of the scale – resolution and volume – there are concerted efforts to link the information from light and electron microscopes through correlative workflows to link structure to function. Here, we consider the status and potential of correlative imaging in the volume domain (3D CLEM).

Highlights

- Correlative light and electron microscopy enhances study of biological systems.
- Integrated microscopes can simplify workflow for 3D-CLEM.
- Automation is key to improve speed and accuracy for large scale 3D-CLEM.

Introduction

To observe a living process in detail, from cell to organism, start to finish, holds much allure in domains of systems biology (e.g., embryology, neurobiology, immunology), yet also poses significant challenges. Living systems organize and evolve in four dimensions, on time and length scales spanning decades from nanoscale to macroscale. Resolution of the smallest features in multi-cellular systems generally pushes the boundaries of optical microscopy into the domain of electron microscopy. Imaging the largest and slowest processes poses a different challenge: microscopy capabilities for imaging volumes more appreciable than single cells have long been limited. Yet, within the past several years, light microscopy (LM) and electron microscopy (EM) have made significant advances at both ends of scale.

Indeed, there are two ongoing revolutions in bioimaging. The first is the 'resolution revolution', which has occurred with respect to spatial scale in both EM and LM. In EM, single particle cryo EM has reached ångström resolution and is becoming competitive to X-ray crystallography for macromolecular structure determination [1, 2]. In LM, the advent of super-resolution techniques that circumvent the Abbe limit have pushed resolution down to 10s of nm [3].

The second is the 'volume revolution', which is again taking place in both EM and LM. In EM, automated block face and array tomography techniques are reaching the millimeter scale at nanometer resolution [4, 5]. In LM, intact deep tissue imaging with two-photon laser scanning microscopy, light sheet microscopy, and tomographic and episcopic microscopies have pushed volume imaging into the scale of model organisms [6, 7].

At both ends of these scale revolutions – resolution and volume – there are concerted efforts to link the information from light and electron microscopes through correlative workflows and instruments. Correlative Light and EM (CLEM) can serve three goals [8]. First, fluorescence expression in LM can be used to pinpoint a region of interest for high-resolution structural EM. Second, the structural images obtained with EM can be placed in the context of live-cell volume LM. Third, an accurate overlay can be made to precisely locate fluorescently-tagged biomolecules within the structural image obtained with EM.

3D CLEM combines volume LM and volume EM to give precise 3D maps of molecular and structural architecture, connecting events taking place over large scales, from dynamic information in the living organism to the smallest structural detail. Below, we will first briefly consider recent developments in volume LM and volume EM separately, and then focus on 3D CLEM. CLEM has seen rapid developments in sample preparation, dedicated workflows, instrumentation, and multi-modal probes (reviewed in [8]). Here, we consider the status, potential, and challenges of correlative imaging in the volume domain.

Light microscopy of volumes

Scattering of light in dense tissue has traditionally limited the sample volume that can be imaged by light microscopy. Owing to significant improvement in biological and chemical probe brightness and

stability [9, 10], as well as focused engineering efforts to combine and optimize instrumentation (see references in [11]), the LM "photon budget" can be split up between spatial and temporal resolution.

In non-transparent living samples, options for increasing the penetration depth are limited. Multi-photon imaging techniques simultaneously offer two benefits: the use of longer wavelengths of light that are scattered less in tissue, and optical sectioning due to the intensity dependence of nonlinear absorption [12]. To obtain the high intensities necessary for multi-photon excitation, fluorescence imaging is typically performed by scanning a focused beam in an epifluorescence geometry (Fig. 1a), similar to confocal microscopy, without need of a pinhole. Modern scanning strategies now make the speed of multi-photon imaging comparable with confocal microscopy. For instance, resonant-scanners can image single plane fields of view at ~30 Hz. Accessing volumes has been made faster by piezo scanners, strategies to alter optical divergence through acousto-optical lenses [13], and remote focusing [14]. Combinations of these technologies in a 2-photon random access microscope have recently reached a mesoscale field of view (5 mm diameter) with subcellular resolution [15].

Planar illumination of the sample using different varieties of light-sheet microscopy (reviewed in [16]) enables images to be gathered with cellular resolution from volumes of nearly 1 mm^3 at rates >3 Hz [17]. The basic principle of light-sheet is to collect fluorescence generated along an axial slice of the illumination cone (Fig. 1b). By removing the epifluorescence detection configuration, the optical paths for illumination and detection can be optimized independently. Fluorescence from the sheet can be imaged simultaneously to a camera (e.g., 4.2 megapixel sCMOS cameras are sensitive enough for functional imaging with frames rates of 100 fps). With high speed and expanded volumes, light sheet microscopes can follow developmental processes in small organisms over several days [6, 18-20], though have so far been limited to transparent samples like *C. elegans*, zebrafish larvae, and *Drosophila* larvae.

Recent developments in both multi-photon and light sheet microscopies have moved towards higher resolution with the help of spatial light modulators (SLMs). SLMs can be used for holographic imaging [21], shaping light into non-diffracting beams (e.g., Bessel beams in lattice light sheet microscopy [22]), extending depth of field [23], correcting optical aberrations [24], and controlling wavefront propagation in opaque samples [25-27].

Both multiphoton and light sheet imaging techniques minimise the dose of high energy visible photons into the sample, thereby limiting photobleaching and phototoxicity. Phototoxicity is not a concern for volume imaging of fixed samples, and instead photostability is key. Depths can be accessed by reducing the scattering potential of the sample by removing dense lipids from membranes prior to imaging (reviewed in [28]) and then applying light-sheet or tomographic imaging techniques [7, 23]. Alternatively, slices of the sample can be removed from the surface, and either the block face can be sequentially imaged (e.g. HREM) or the slices can be sequentially imaged (array tomography) and the resulting stack of images reconstructed into a digital volume [29, 30].

Electron microscopy of volumes

Scattering of electrons in matter is more severe than scattering of photons, and so the sample volume that can be imaged by electron microscopy is even more limited. Resin-embedded tissues

must be cut into ultrathin sections of 50–100 nm for imaging in the transmission EM (TEM). Electron tomography can be used to reconstruct a high resolution volume through a thin section of 200 nm – 1 µm. Imaged volumes can be increased by cutting and imaging serial ultrathin sections, demonstrated in the first large-scale study of the complete neural network in *C. elegans* [31, 32]. Recently, automation of sample loading and advances in the TEM and detector arrays have delivered a complete EM volume of the adult *Drosophila melanogaster* brain [33].

Serial sections can also be imaged in the scanning EM (SEM) in a process known as array tomography. Automation of serial section collection onto kapton tape, which is then placed onto wafers and imaged in an SEM, has delivered large volume reconstructions of mouse neocortex [34] and a whole zebrafish brain [35]. Maintaining the library of sections on a wafer is advantageous as it allows re-inspection of the sections and thus sequential steps of low-magnification pre-scanning with higher-magnification re-scanning of targeted sections or areas. This is crucial to achieve sufficient throughput with inherently slow single-beam SEM. For instance, the serial sectioning of a 5.5-day old zebrafish brain performed by Hildebrand et al. resulted in 17,963 sections at about 60 nm section thickness [35]. Low resolution (758.8 x 758.8 nm^2) overview scanning of all sections lasted ~5 days, followed by two runs of ~100 days at higher resolution (56.4 x 56.4 nm^2 and 18.8 x 18.8 nm^2) scanning, each of several Terabytes data size. Finer structural details, such as synaptic connections, were then evaluated by further inspection at 4 x 4 nm^2 pixel size. These acquisition times can be considerably reduced with recently reported multi-beam scanning electron microscopes [34, 36], which can operate with up to 196 beams scanning in parallel [37], providing a breakthrough, particularly for array tomography.

In other volume EM techniques the sections are discarded, and instead the blockface is imaged after each cut, with an integrated microtome, referred to as Serial Block Face SEM (SBF-SEM or SBEM), or with a Focused Ion Beam (FIB-SEM). All EM sample preparation steps (fixation, plastic embedding, staining, and sectioning) lead to distortions, which alter intra-sample coordinates compared to those observed before EM preparation. However, after sectioning, the (two-dimensional) coordinate transformation imposed by the sectioning may be different for each section. Thus, while serial sectioning involves careful non-linear section-to-section registration [35], blockface techniques deliver aligned high-resolution image stacks through large volumes. Indeed, SBEM and FIB-SEM have both already been used to image volumes of brain and other tissues [38-41].

Correlative microscopy of volumes

3D CLEM is generally performed with the aim of locating a region of interest within a large, potentially live, sample, from which the structural information is harvested. This targeted approach to electron microscopy combines information on the identity and provenance of cells of interest from LM, with their structure, niche and context from EM. The workflow for this type of correlation, schematically indicated in the upper part of Fig. 2, is usually 3D LM, followed by sample preparation, followed by 3D EM, alignment of the two image stacks, 3D modelling and visualisation of the data, and relocation and analysis of the structure of the cells of interest [42].

There are several challenges associated with this workflow, above and beyond the challenge of imaging volumes in both modalities:

The first challenge is tracking the region of interest from LM to EM. Several tools have been developed in response. An X-ray microscopy step can be inserted between LM and EM, using microCT to 'see' inside the intact sample and measure the position of the region of interest for targeted trimming and analysis by EM [43]. Furthermore, powerful lasers can be used to create physical marks close to the cells of interest via infrared branding, which can be visualised in both microCT and EM, giving 3D spatial maps to navigate to target structures [44, 45]. Photo- and chemically-convertible tags (e.g. miniSOG [46], APEX [47]) can also be detected in both microCT and EM and can be used to confirm the identity of the region of interest across multiple imaging modalities [48].

The second challenge is in the overlay of 3D image data from different imaging modalities, each of which has different contrast mechanisms (fluorescence emission, electron dense membranes), sample properties (geometry, distortions) and image properties (pixel size, lateral resolution, axial resolution). Software solutions are being developed, in the form of software that aids visualisation and alignment of large 3D image data, including the FIJI plugins TrakEM2 [49], BigDataViewer [50] and BigWarp [51], and ec-CLEM [52] on the ICY platform. These algorithms depend on manual identification of matching landmarks within the datasets for alignment, and can only work to an accuracy that is determined by the extent of the sample distortions caused by intermediate sample preparation steps.

A more challenging correlative workflow, indicated in the lower panel of Fig. 2, aims to localise macromolecules to subcellular compartments *in situ* in cells and tissues. These experiments are more challenging, because the region of interest is orders of magnitude smaller than in the approach described above, and thus the demands on resolution, tracking and overlay accuracy are increased. New approaches to sample preparation for correlative imaging have the potential to aid this workflow. Rather than performing LM prior to fixation and embedding for EM, the fluorescence of LM probes is either preserved during preparation for imaging in EM (see [8] for references), or sections are immunolabelled with a fluorescent moiety [53], so that both imaging modalities are performed on the exact same sample. Serial sections with both electron dense stains and fluorescent labels may be imaged sequentially in separate fluorescence and electron microscopes [54-56], or *in situ* inside integrated light and electron microscopes [57, 58]. These techniques have not yet been applied routinely to larger tissue samples, and compromises tend to be made on both fluorescence intensity and electron contrast in the sample, but the technique has the potential to produce high (super) resolution macromolecular localisations within easily-aligned [58] 3D image stacks from both imaging modalities.

What is next? Size, speed, and accuracy

With LM, instrumentation is in place to follow biomolecular dynamics during development in embryos or small animals, provided sufficient sample transparency. Live LM imaging in non-transparent organisms with LM is advancing with development of biologically compatible near-infrared probes [59], longer wavelengths more optimal for penetrating tissues [60], and photoacoustic modalities [61]. A broader set of biological systems can be studied *in vitro*, where larger samples can be made transparent by extracting lipids to reduce photon scattering. However, in

terms of correlation with volume EM, it is not clear whether such clearing techniques are compatible with good ultrastructural preservation and morphology in EM. Compatibility of tissue clearing with EM sample preparation and ultrastructural preservation needs to be a strong point of attention for bringing techniques like light sheet microscopy in 3D CLEM.

Still, with volume EM, only orders of magnitude smaller volumes are within reach, necessitating selection of a manageable block based on the LM data. For mm^3-sized blocks this is straightforward, but selection of smaller blocks for block-face 3D CLEM, needs labour-intensive intermediate steps. Serial sectioning can be performed in automated fashion, but scanning the larger sample size is currently a bottleneck consuming more time than the block-face approach. Multi-beam SEMs [36, 37] allow parallelized data collection, leading to acquisition of tens of Terabytes datasets well within one day. Simplification and automation of sample preparation and image acquisition processes is not only needed to increase throughput and volume size, but would also increase reproducibility. Data collection can be optimized via smart tracking algorithms that detect features, landmarks, or probes identified by LM or X-ray microscopy to drive data collection from regions of interest for EM. Array tomography approaches have already used low-resolution EM pre-scanning to determine regions for higher resolution re-scanning [34, 35]. With its large specificity and ease of recognition, fluorescence seems optimally suited for fast identification of target areas using an integrated microscope. Further development of sample preparation protocols that allow fluorescence preservation within the sections, or post-sectioning immunolabelling are therefore key to enable fast machine-based scanning decisions. In vivo marking using photoactivatable probes could facilitate workflow where cells can be assessed for function, marked optically, found by LM, and reconstructed by CLEM, but this may be depth-limited for larger samples.

In both LM and EM, larger data sets lead to challenges in data transfer, storage, and analysis. For light-sheet microscopy, data sets are already reaching Petabytes sizes. Thus, notably for LM, analysis software and workflows [62, 63] are increasingly available, paving the way for volume EM and 3D CLEM. In addition, shared online availability of open access large data sets will boost analysis by researchers without access to advanced microscopy or sample preparation [64, 65], but especially for 3D CLEM needs careful consideration and uniform definitions for metadata, which for correlated data sets are not yet existing. For high resolution LM-EM overlaid data sets this also needs consideration of the way these data sets are represented.

To increase accuracy and allow recording of ultrastructural maps coloured at near-EM resolution with molecular content, e.g. indicated by in-section fluorescent probes, serial sectioning intrinsically offers high-resolution fluorescence localization in the axial direction. Development and automation of integrated array tomography brings fast acquisition by fluorescence-guided scanning paired with high accuracy localization [58], with super-resolution LM [57] providing additional lateral localization accuracy.

The last mile problem

Will 3D ultrastructural maps from volume EM, annotated by LM maps of molecular markers or cellular function measured in a well-defined live context, transform the study of biology at the organism scale? Likely. In LM, remarkably, registration of volumetrically morphed confocal z-stacks

has allowed mapping of anatomy of populations of age-matched individual zebrafish larvae with near cellular resolution [66]. Registration with EM volume maps [35] may raise the possibility of comparisons of macroscopic distributions of ultrastructural features between individual animals. However, certain classes of problems are inherently difficult to address at the population level. For example, in the brain, while the projectome may turn out to be comparable between individuals, connectomes are likely to vary at the level of individual synapses. Importantly, the work of Hildebrand et al. [35] demonstrates the feasibility of taking an individual animal through a full workflow including functional imaging to serial section SEM. Further optimization of a pipeline for 3D CLEM and integrated workflows will push correlative measurements in biological systems to even richer meta datasets.

Acknowledgements

This work was supported by the Francis Crick Institute which receives its core funding from Cancer Research UK (FC001999), the UK Medical Research Council (FC001999), and the Wellcome Trust (FC001999); and by the Netherlands Organization for Scientific Research (NWO) through the STW Perspectief program Microscopy Valley.

Competing financial interest

JPH is co-founder of and shareholder in Delmic BV, a company selling integrated microscopes.

References

1. Kuhlbrandt, W., *Biochemistry. The resolution revolution.* Science, 2014. **343**(6178): p. 1443-4.
2. Bai, X.-c., G. McMullan, and S.H.W. Scheres, *How cryo-EM is revolutionizing structural biology.* Trends in Biochemical Sciences, 2015. **40**(1): p. 49-57.
3. Sydor, A.M., et al., *Super-resolution microscopy: from single molecules to supramolecular assemblies.* Trends in cell biology, 2015. **25**(12): p. 730-748.
4. Briggman, K.L. and D.D. Bock, *Volume electron microscopy for neuronal circuit reconstruction.* Curr Opin Neurobiol, 2012. **22**(1): p. 154-61.
5. Peddie, C.J. and L.M. Collinson, *Exploring the third dimension: Volume electron microscopy comes of age.* Micron, 2014. **61**: p. 9-19.
- 6. Chhetri, R.K., et al., *Whole-animal functional and developmental imaging with isotropic spatial resolution.* Nat Methods, 2015. **12**(12): p. 1171-8.
7. Susaki, E.A. and H.R. Ueda, *Whole-body and Whole-Organ Clearing and Imaging Techniques with Single-Cell Resolution: Toward Organism-Level Systems Biology in Mammals.* Cell Chem Biol, 2016. **23**(1): p. 137-57.
- 8. Boer, P. de, J.P. Hoogenboom, and B.N.G. Giepmans, *Correlated light and electron microscopy: ultrastructure lights up!* Nature Methods, 2015. **12**: p. 503-513.
9. Lavis, L.D., *Teaching Old Dyes New Tricks: Biological Probes Built from Fluoresceins and Rhodamines.* https://doi.org/10.1146/annurev-biochem-061516-044839, 2017.
10. Germond, A., et al., *Design and development of genetically encoded fluorescent sensors to monitor intracellular chemical and physical parameters.* Biophysical Reviews, 2016. **8**(2): p. 121-138.

●● 11. Yang, W. and R. Yuste, *In vivo imaging of neural activity.* Nat Meth, 2017. **14**(4): p. 349-359.
12. Denk, W. and K. Svoboda, *Photon Upmanship: Why Multiphoton Imaging Is More than a Gimmick.* Neuron, 1997. **18**(3): p. 351-357.
13. Katona, G., et al., *Fast two-photon in vivo imaging with three-dimensional random-access scanning in large tissue volumes.* Nat Meth, 2012. **9**(2): p. 201-208.
14. Botcherby, E.J., et al., *An optical technique for remote focusing in microscopy.* Optics Communications, 2008. **281**(4): p. 880-887.
●● 15. Sofroniew, N.J., et al., *A large field of view two-photon mesoscope with subcellular resolution for in vivo imaging*, in *eLife*. 2016.
●● 16. Power, R.M. and J. Huisken, *A guide to light-sheet fluorescence microscopy for multiscale imaging.* Nat Meth, 2017. **14**(4): p. 360-373.
17. Ahrens, M.B. and F. Engert, *Large-scale imaging in small brains.* Current opinion in neurobiology, 2015. **32**: p. 78-86.
18. Tomer, R., et al., *Quantitative high-speed imaging of entire developing embryos with simultaneous multiview light-sheet microscopy.* Nat Methods, 2012. **9**(7): p. 755-63.
19. Vladimirov, N., et al., *Light-sheet functional imaging in fictively behaving zebrafish.* Nature Methods, 2014. **11**(9): p. 883-884.
20. Dunn, T.W., et al., *Brain-wide mapping of neural activity controlling zebrafish exploratory locomotion.* eLife, 2016. **5**: p. e12741.
21. Pozzi, P., et al., *High-throughput spatial light modulation two-photon microscopy for fast functional imaging.* Neurophotonics, 2015. **2**(1): p. 015005-015005.
●● 22. Chen, B.-C., et al., *Lattice light-sheet microscopy: Imaging molecules to embryos at high spatiotemporal resolution.* Science, 2014. **346**(6208).
● 23. Tomer, R., et al., *SPED Light Sheet Microscopy: Fast Mapping of Biological System Structure and Function.* Cell, 2015. **163**(7): p. 1796-1806.
●● 24. Ji, N., *Adaptive optical fluorescence microscopy.* Nat Meth, 2017. **14**(4): p. 374-380.
25. ChaigneT, et al., *Controlling light in scattering media non-invasively using the photoacoustic transmission matrix.* Nat Photon, 2014. **8**(1): p. 58-64.
26. Cui, J.-H.P., S. Wei, and Meng, *High-resolution in vivo imaging of mouse brain through the intact skull.* 2015.
27. N'Gom, M., et al., *Controlling Light Transmission Through Highly Scattering Media Using Semi-Definite Programming as a Phase Retrieval Computation Method.* Scientific Reports, 2017. **7**(1): p. 2518.
● 28. Silvestri, L., et al., *Clearing of fixed tissue: a review from a microscopist's perspective.* Journal of Biomedical Optics, 2017. **21**(8): p. 081205-081205.
29. Nanguneri, S., et al., *Three-dimensional, tomographic super-resolution fluorescence imaging of serially sectioned thick samples.* PLoS One, 2012. **7**(5): p. e38098.
30. Norris, F.C., et al., *A coming of age: advanced imaging technologies for characterising the developing mouse.* Trends Genet, 2013. **29**(12): p. 700-11.
31. White, J., et al., *The structure of the nervous system of the nematode C.elegans.* Philos Trans R Soc Lond B Biol Sci, 1986(314): p. 1-340.
32. Emmons, S.W., *The beginning of connectomics: a commentary on White et al. (1986) 'The structure of the nervous system of the nematode Caenorhabditis elegans'.* Philos Trans R Soc Lond B Biol Sci, 2015. **370**(1666).
●● 33. Zheng, Z., et al., *A Complete Electron Microscopy Volume Of The Brain Of Adult Drosophila melanogaster.* bioRxiv, 2017.
● 34. Kasthuri, N., et al., *Saturated Reconstruction of a Volume of Neocortex.* Cell, 2015. **162**(3): p. 648-61.
●● 35. Hildebrand, D.G.C., et al., *Whole-brain serial-section electron microscopy in larval zebrafish.* Nature, 2017. **545**: p. 345-349.
● 36. Eberle, A.L., et al., *High-resolution, high-throughput imaging with a multibeam scanning electron microscope.* Journal of Microscopy, 2015. **259**(2): p. 114-120.

● 37. Ren, Y. and P. Kruit, *Transmission electron imaging in the Delft multibeam scanning electron microscope 1.* Journal of Vacuum Science & Technology B, Nanotechnology and Microelectronics: Materials, Processing, Measurement, and Phenomena, 2016. **34**(6): p. 06KF02.

38. Denk, W. and H. Horstmann, *Serial block-face scanning electron microscopy to reconstruct three-dimensional tissue nanostructure.* PLoS Biol, 2004. **2**(11): p. e329.

39. Knott, G., S. Rosset, and M. Cantoni, *Focussed ion beam milling and scanning electron microscopy of brain tissue.* J Vis Exp, 2011(53).

40. Narayan, K. and S. Subramaniam, *Focused ion beams in biology.* Nat Methods, 2015. **12**(11): p. 1021-31.

41. Xu, C.S., et al., *Enhanced FIB-SEM systems for large-volume 3D imaging.* Elife, 2017. **6**.

●● 42. Karreman, M.A., et al., *Intravital Correlative Microscopy: Imaging Life at the Nanoscale.* Trends Cell Biol, 2016. **26**(11): p. 848-863.

● 43. Karreman, M.A., et al., *Fast and precise targeting of single tumor cells in vivo by multimodal correlative microscopy.* J Cell Sci, 2016. **129**(2): p. 444-56.

44. Clark, S.J., et al., *Mapping the differential distribution of glycosaminoglycans in the adult human retina, choroid, and sclera.* Invest Ophthalmol Vis Sci, 2011. **52**(9): p. 6511-21.

45. Maco, B., et al., *Correlative in vivo 2 photon and focused ion beam scanning electron microscopy of cortical neurons.* PLoS One, 2013. **8**(2): p. e57405.

46. Shu, X., et al., *A Genetically Encoded Tag for Correlated Light and Electron Microscopy of Intact Cells, Tissues, and Organisms.* Plos Biology, 2011. **9**(4).

47. Lam, S.S., et al., *Directed evolution of APEX2 for electron microscopy and proximity labeling.* Nat Methods, 2015. **12**(1): p. 51-4.

48. Bushong, E.A., et al., *X-ray microscopy as an approach to increasing accuracy and efficiency of serial block-face imaging for correlated light and electron microscopy of biological specimens.* Microsc Microanal, 2015. **21**(1): p. 231-8.

49. Schindelin, J., et al., *Fiji: an open-source platform for biological-image analysis.* Nat Methods, 2012. **9**(7): p. 676-82.

● 50. Pietzsch, T., et al., *BigDataViewer: visualization and processing for large image data sets.* Nat Meth, 2015. **12**(6): p. 481-483.

● 51. Bogovic, J.A., et al. *Robust registration of calcium images by learned contrast synthesis*. in *2016 IEEE 13th International Symposium on Biomedical Imaging (ISBI)*. 2016.

52. Paul-Gilloteaux, P., et al., *eC-CLEM: flexible multidimensional registration software for correlative microscopies.* Nat Methods, 2017. **14**(2): p. 102-103.

53. Kuipers, J., P. de Boer, and B.N. Giepmans, *Scanning EM of non-heavy metal stained biosamples: Large-field of view, high contrast and highly efficient immunolabeling.* Exp Cell Res, 2015. **337**(2): p. 202-7.

54. Kopek, B.G., et al., *Correlative photoactivated localization and scanning electron microscopy.* PLoS One, 2013. **8**(10): p. e77209.

55. Collman, F., et al., *Mapping synapses by conjugate light-electron array tomography.* J Neurosci, 2015. **35**(14): p. 5792-807.

56. Kim, D., et al., *Correlative stochastic optical reconstruction microscopy and electron microscopy.* PLoS One, 2015. **10**(4): p. e0124581.

● 57. Peddie, C.J., et al., *Correlative super-resolution fluorescence and electron microscopy using conventional fluorescent proteins in vacuo.* J Struct Biol, 2017. **199**(2): p. 120-131.

● 58. Haring, M.T., et al., *Automated sub-5nm image registration in integrated correlative fluorescence and electron microscopy using cathodoluminescence pointers.* Scientific Reports, 2017. **7**: p. 43621.

59. Hong, G., A.L. Antaris, and H. Dai, *Near-infrared fluorophores for biomedical imaging.* 2017. **1**: p. 0010.

60. Ouzounov, D.G., et al., *In vivo three-photon imaging of activity of GCaMP6-labeled neurons deep in intact mouse brain.* Nat Methods, 2017. **14**(4): p. 388-390.

61. Xia, J., J. Yao, and L.V. Wang, *Photoacoustic tomography: principles and advances.* Electromagn Waves (Camb), 2014. **147**: p. 1-22.
62. Freeman, J., et al., *Mapping brain activity at scale with cluster computing.* Nature methods, 2014. **11**(9): p. 941-950.
63. Amat, F., et al., *Efficient processing and analysis of large-scale light-sheet microscopy data.* Nat Protoc, 2015. **10**(11): p. 1679-96.
64. Iudin, A., et al., *EMPIAR: a public archive for raw electron microscopy image data.* Nat Methods, 2016. **13**(5): p. 387-8.
65. Williams, E., et al., *The Image Data Resource: A Bioimage Data Integration and Publication Platform.* Nat Methods, 2017. **14**(8): p. 775-781.
66. Randlett, O., et al., *Whole-brain activity mapping onto a zebrafish brain atlas.* Nat Meth, 2015. **12**(11): p. 1039-1046.

BOX 1. Techniques and their abbreviations

LM: Light microscopy

EM: Electron microscopy

TEM: Transmission electron microscopy

SEM: Scanning electron microscopy

CLEM: Correlative light electron microscopy

MPM: multiphoton microscopy

SPIM: selective planar illumination microscopy, another name for light sheet microscopy

SBEM / SBF SEM: Serial blockface SEM

FIB SEM: focused ion beam SEM

microCT: micro computed tomography, of X-ray microtomography

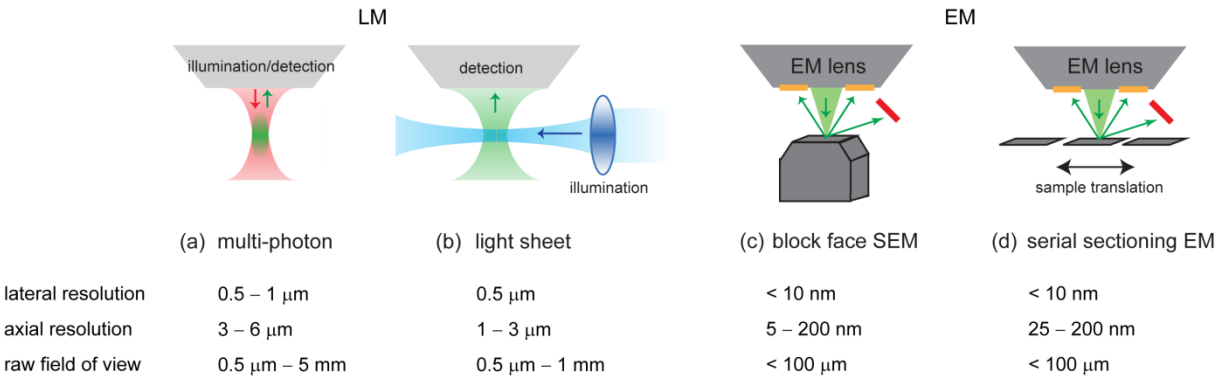

Figure 1. Schematics of basic principles behind volume imaging techniques in LM and EM, with typical resolution and volumetric benchmarks. (a) Multi-photon light microscopy typically uses an epifluorescence geometry. Optical sectioning depends on the size of the nonlinear focus. (b) Light-sheet microscopy typically decouples the illumination and detection optical paths. Optical sectioning depends on the thickness of the light sheet. (c) In block-face SEM, the resin block containing the sample after fixation, embedding, and staining, is placed in the SEM in its entirety. After imaging, the upper face of the block is removed using an integrated microtome or a focused ion beam, followed by another image acquisition. (d) Alternatively, in serial section EM or array tomography, the resin block is fully sectioned prior to imaging, with all sections being collected in single file automatically. These files of sections are then loaded into the SEM for sequential scanning. Note that lateral resolution values are typical best obtained, which especially in SEM can be easily adjusted to lower resolution leading to larger raw fields of view, e.g. for overview imaging as used in [34].

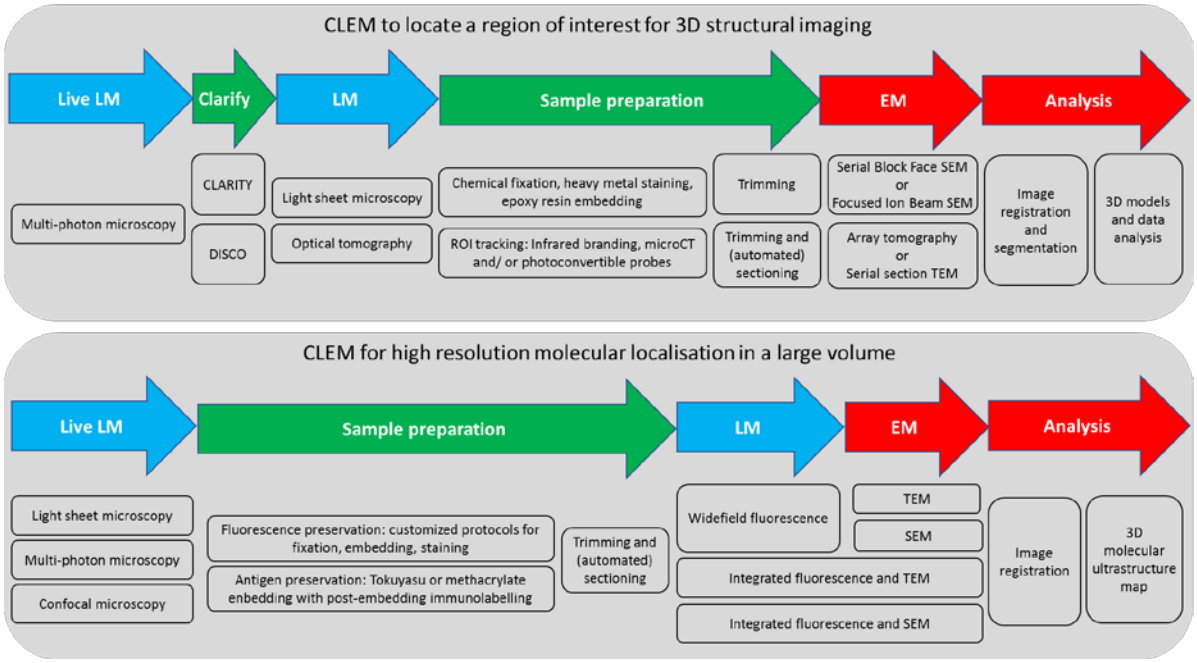

Figure 2. Alternative schematic workflows for correlative light and electron microscopies, starting from biological samples labeled with genetically encoded fluorophores. Blue arrows indicate LM steps, green sample preparation and intermediate steps, red arrows EM and 3D analysis and reconstruction. The upper workflow depicts 3D CLEM where structural information is obtained from a targeted region of interest that is first identified with LM on a large, potentially live, sample. Lower workflow indicates 3D CLEM where the aim is to obtain a high resolution 3D map of macromolecular positions within the 3D ultrastructure. Note that these workflows serve as a general guideline and illustration, where individual steps can or need to be omitted depending on the type of sample and specific goal of the experiments. Considerations are given in the text and referred to materials.